J. exp. Biol. ***189****, 133–161 (1994)*
Printed in Great Britain © The Company of Biologists Limited 1994

KINEMATICS OF PECTORAL FIN LOCOMOTION IN THE BLUEGILL SUNFISH *LEPOMIS MACROCHIRUS*

ALICE C. GIBB[1], BRUCE C. JAYNE[2] AND GEORGE V. LAUDER[1]

[1]*Department of Ecology and Evolutionary Biology, University of California, Irvine, CA 92717, USA* and [2]*Department of Biological Sciences, University of Cincinnati, Cincinnati, OH 45221-0006, USA*

Accepted 6 December 1993

Summary

The pectoral fins of ray-finned fishes are flexible and capable of complex movements, and yet little is known about the pattern of fin deformation during locomotion. For the most part, pectoral fins have been modeled as rigid plates. In order to examine the movements of different portions of pectoral fins, we quantified the kinematics of pectoral fin locomotion in the bluegill sunfish *Lepomis macrochirus* using several points on the distal fin edge and examined the effects of swimming speed on fin movements. We simultaneously videotaped the ventral and lateral views of pectoral fins of four fish swimming in a flow tank at five speeds ranging from 0.3 to 1.1 total lengths s^{-1}. Four markers, placed on the distal edge of the fin, facilitated field-by-field analysis of kinematics. We used analyses of variance to test for significant variation with speed and among the different marker positions. Fin beat frequency increased significantly from 1.2 to 2.1 Hz as swimming speed increased from 0.3 to 1.0 total lengths s^{-1}. Maximal velocities of movement for the tip of the fin during abduction and adduction generally increased significantly with increased swimming speed. The ratio of maximal speed of fin retraction to swimming speed declined steadily from 2.75 to 1.00 as swimming speed increased. Rather than the entire distal edge of the fin always moving synchronously, markers had phase lags as large as 32 ° with respect to the dorsal edge of the fin. The more ventral and proximal portions of the fin edge usually had smaller amplitudes of movement than did the more dorsal and distal locations. With increased swimming speed, the amplitudes of the lateral and longitudinal fin movements generally decreased. We used two distal markers and one basal reference point to determine the orientation of various planar fin elements. During early adduction and most of abduction, these planar fin elements usually had positive angles of attack. Because of fin rotation, angles of attack calculated from three-dimensional data differed considerably from those estimated from a simple lateral projection. As swimming speed increased, the angles of attack of the planar fin elements with respect to the overall direction of swimming approached zero. The oscillatory movements of the pectoral fins of bluegill suggest that both lift- and drag-based propulsive mechanisms are used to generate forward thrust. In addition, the reduced frequency parameter calculated for the pectoral fin of *Lepomis* (σ=0.85) and the

Key words: locomotion, fish, swimming, kinematics, pectoral fin, speed, bluegill sunfish, *Lepomis macrochirus*.

Reynolds number of 5×10^3 indicate that acceleration reaction forces may contribute significantly to thrust production and to the total force balance on the fin.

Introduction

Pectoral fin swimming is one of the most important modes of locomotion for ray-finned fishes. In addition to being the primary mode of locomotion for several large families of teleost fishes (Lindsey, 1978), it is used by most ray-finned species for maneuvering and swimming at low speeds. Despite the critical importance of this method of locomotion to fishes, most research on fish locomotion has focused on caudal fin and body swimming. Only a handful of investigators (Webb, 1973; Blake, 1979, 1980; Geerlink, 1983, 1989; Archer and Johnston, 1989) have described fin movements during pectoral fin swimming.

Webb and Blake (1985), in a review of fish locomotion, suggested that oscillating locomotor movements of fish pectoral fins involve primarily either a drag-based or a lift-based mechanism to produce thrust. During drag-based propulsion, the fin is pulled posteriorly through the water like a paddle, with its surface perpendicular to the direction of movement. Lift-based pectoral fin propulsors may use their fins as wings with predominantly dorso-ventral movements and a fin surface oriented obliquely with respect to movement (Webb and Blake, 1985). In addition to lift- and drag-based mechanisms, the acceleration reaction is another mechanism which may contribute to forward thrust during pectoral fin locomotion (Daniel, 1984; Daniel and Webb, 1987; Webb, 1988). The acceleration reaction is force generated by resistance of the fluid surrounding the fin in response to changes in velocity of the fin. The acceleration reaction is especially important during periods of unsteady flow (Daniel, 1984).

Most of the work examining the mechanisms of thrust production during pectoral fin locomotion has been theoretical (Blake, 1979, 1980). Blake (1979, 1980) and Webb (1973, 1975) have provided the most comprehensive kinematic data available, but there is still a lack of certain kinematic information that is critical for understanding the mechanisms of fin-based propulsion. For example, because the displacements and velocities of discrete points along the trailing edge of the fin have not been determined, it is unclear to what extent a fin may function as a rigid paddle. Furthermore, the relative amounts of dorso-ventral and antero-posterior movement during pectoral fin locomotion have not yet been quantified, and there are no data describing the relative contributions of each of the orthogonal displacements to the overall fin movement. Determining whether fish use lift- or drag-based propulsion during pectoral fin locomotion has been difficult.

The effects of speed on pectoral fin movements have also received little attention (for an exception, see Webb, 1973). Most tetrapods change limb kinematics when changing from a walk to a run (Hildebrand, 1985). Similarly, fish that swim using their pectoral fins may change the pattern of fin movement as speed increases. Fish in the family Embiotocidae may use a different fin movement pattern at different swimming speeds (Webb, 1973), but no data are available for more generalized teleosts.

Visualizing the edges of the pectoral fin has been a significant technical problem in previous studies. The combination of the membranous nature of the fin and the lack of contrast between the fish's body and its pectoral fins makes observing movements of the

pectoral fin from a lateral view difficult. Most studies have concentrated on a ventral view of pectoral fin locomotion, and three-dimensional calculations of displacement have been difficult if not impossible. To overcome some of these shortcomings, we employed a marking technique for the distal edge of the pectoral fin.

The aims of this study were to describe the movements of the pectoral fins during locomotion in both lateral and ventral view (allowing a three-dimensional analysis) and to examine the effects of changes in speed on fin kinematics. In addition, to evaluate whether bluegill sunfish use a lift, drag or acceleration reaction-based mechanism of pectoral fin propulsion, we examined movements of the fin with respect to fluid flow to determine whether fin movements conformed to *a priori* hydrodynamic expectations for these locomotor modes (Daniel, 1984; Webb and Blake, 1985).

Materials and methods

Animals

Bluegill sunfish (*Lepomis macrochirus* Rafinesque) were chosen for their relatively generalized body and fin shapes (compared with fish that are specialized for anguilliform or labriform swimming, for example) and because of their propensity to swim using their pectoral fins at low speeds. Fish were collected from fish ponds near Fresno, California, held in freshwater aquaria at 20 °C, and fed earthworms twice weekly. We selected individuals of similar length in order to minimize size effects. Morphological variables for the four individuals used in this study are summarized in Table 1.

Experimental protocol

Five swimming speeds were examined: 0.3, 0.5, 0.75, 1.0 and 1.1 total lengths per second ($TL\,s^{-1}$). These speeds were chosen because they represent the range of speeds over which bluegill use their pectoral fins for locomotion. At speeds greater than $1.1\,TL\,s^{-1}$, bluegill begin to use body and caudal fin locomotion in addition to, or in place of, pectoral fin locomotion. Each individual used in the study was filmed swimming at all five speeds. For all individuals, four consecutive fin beats were analyzed at each speed.

Bluegill were filmed swimming in a flow tank using a NAC two-camera high-speed video system at 200 fields per second. The flow tank contained approximately 100 l of fresh water and had a working area 45 cm long × 18 cm wide × 18 cm high. Flow speed was controlled by a variable-speed motor attached to a propeller. The fish were filmed from the lateral view through a camera positioned perpendicular to the side of the flow tank. Fish were also filmed simultaneously from the ventral view using a front-surface mirror mounted at an angle to the bottom of the working section.

Before the fish were filmed swimming, four points on the distal edge of the pectoral fin were marked to facilitate motion analysis. Fish were anesthetized using tricaine methanesulfonate, and small black plastic markers (approximately 0.2 cm×0.3 cm) were attached to the left pectoral fin at the most dorsal, most ventral and two intermediate locations on the distal edge of the fin (Fig. 1) using cyanoacrylate adhesive glue. The fish were then returned to the flow tank and allowed to recuperate from the anesthesia for at least 1 h before they were filmed.

Table 1. *Summary of morphological variables measured on bluegill sunfish used in this study*

Individual	Mass (g)	Total length (cm)	Standard length (cm)	Fin area (cm^2)	Distance to marker from fin base (cm)				Ray number with marker			
					4	3	2	1	4	3	2	1
5	109	18.07	14.81	6.49	4.31	3.90	3.09	2.13	4	6	8	10
11	85	17.72	14.86	5.95	4.18	3.41	2.53	1.88	4	6	8	10
26	105	17.70	14.99	6.02	4.10	3.55	2.52	1.77	3	6	8	10
27	106	18.03	15.04	6.09	4.18	3.70	2.55	1.92	3	5	8	10

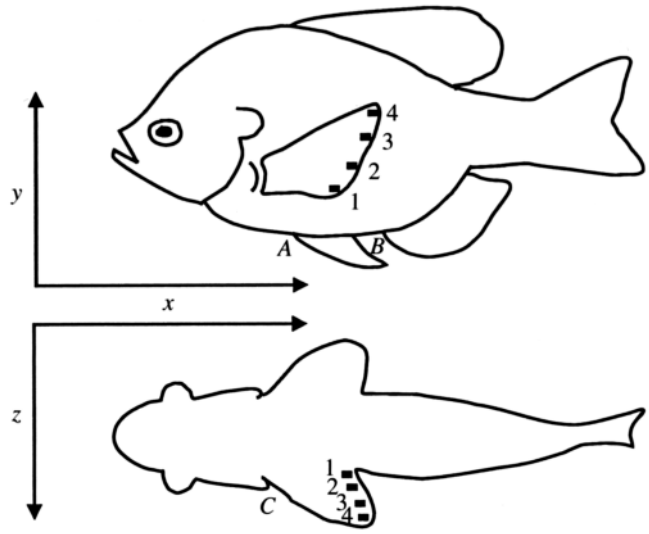

Fig. 1. Schematic representation of *Lepomis macrochirus* as videotaped swimming in a flow tank. The upper panel represents the lateral view of the fish. The lower panel is the ventral view through a mirror; hence, the lower marked fin is actually the left fin as indicated in the top panel. Fin markers are indicated by the numbers 1–4 (from ventral to dorsal). The letters *A* (anterior point of attachment of pelvic fins), *B* (anterior point of attachment of anal fin) and *C* (base of left pectoral fin) indicate reference points on the body of the fish. We used the lateral view to measure the longitudinal (*x*) and vertical (*y*) movements, whereas the ventral view coordinates were used primarily to determine lateral (*z*) movements. Note that the lateral view represents the fin before the beginning of abduction, whereas the ventral view illustrates the fin as it would be during the middle of abduction. The fin has been shown in this manner to illustrate best the placement of the markers in both views.

Special care was taken during filming to obtain sequences in which the fish closely matched (±5 %) flow speed (and was thus nearly stationary relative to a fixed frame of reference) for four successive fin beats. In order to minimize potential effects of the tank walls on the flow around the fish (Webb, 1993), we selected only sequences in which the fish was at least 3 cm above the bottom of the flow tank, 6 cm below the surface of the water and very nearly in the center of the working section (fish body more than 5 cm from each wall, and extended fins more than 2 cm from each wall). Qualitative comparisons between the motion of the marked fin with the contralateral unmarked fin revealed no conspicuous differences in the movements.

Image analysis

The video sequences were digitized using a customized microcomputer video analysis program. The four markers on the distal edge of the pectoral fin (Fig. 1) were digitized in both the lateral and the ventral view. In the lateral view, *x* and *y* coordinates were measured for each point, and in the ventral view *x* and *z* coordinates were obtained. In addition to the markers, two reference points on the fish's body were also digitized in each frame. In the lateral view, *x* and *y* reference coordinates were taken for the anterior

points of attachment for the pelvic fins (Fig. 1, point *A*) and anal fin (Fig. 1, point *B*). In the ventral view, the point of attachment of the left pectoral fin to the body (Fig. 1, point *C*) was digitized in order to obtain *x* and *z* reference coordinates. Approximately 20 video frames (at equal time intervals within each sequence) were digitized for each fin beat. Thus, approximately 1600 video frames were analyzed in this study. The resulting coordinates were transferred to a spreadsheet program for the calculation of kinematic variables and further analysis.

Kinematic variables

The markers were identified consecutively from ventral to dorsal as 1, 2, 3 and 4, respectively (Fig. 1). Anterior (protraction) and posterior (retraction) marker movements were defined as movement in the *x* dimension. Dorsal (levation) and ventral (depression) movements were in the *y* dimension. Medial (adduction) and lateral (abduction) movements were in the *z* dimension (Fig. 1), and one fin beat cycle was defined as the time between successive points of maximal lateral excursion of marker 4. This allows the most accurate measurement of cycle duration because there was a relatively sharp peak in displacement curves at maximal lateral displacement. However, the verbal description of the fin beat cycle in the Results and Discussion sections starts at the beginning of abduction to facilitate the qualitative descriptions of fin movement beginning with the time when the fin is located against the body.

Twelve displacement variables were calculated for each fin beat. For all four markers, we calculated the *x*, *y* and *z* excursions as the difference between maximum and minimum values of one fin beat cycle, and these twelve variables were identified by the marker number and the dimension of the excursion (1XEX, 2YEX, 3ZEX, etc.).

For each fin beat, we inverted cycle duration to determine the frequency (FREQ, in Hz). Six variables described the maximum velocities of movement of marker 4 during abduction (ABDMINX, ABDMINY, ABDMINZ) and adduction (ADDMAXX, ADDMAXY, ADDMAXZ) of the fin within each cycle. These velocities equaled the magnitude of marker displacement (in one dimension) divided by the time between successive images. Velocities calculated for abduction were defined as negative values because the direction of movement of the fin during this portion of the fin beat cycle was opposite to the direction of movement of the fish through the water.

We calculated the difference between the time of maximum lateral (*z*) displacement for marker 4 and that of the more ventral markers, divided by cycle duration, and converted the result to degrees (with a 360 ° total cycle duration). These three variables described phase lags between markers 3 and 4, 2 and 4 and 1 and 4, such that positive values indicate that maximum lateral displacement of the more ventral marker followed that of marker 4.

Statistical analyses

Statistical analyses used the SuperANOVA, Statview and Systat programs for Apple Macintosh computers. The primary analysis of the displacement variables was a three-way analysis of variance (ANOVA) in which the main effects were speed, marker and individual. Speed (five levels: 0.3, 0.5, 0.75, 1.0 and 1.1 TL s^{-1}) and marker (four levels:

markers 1, 2, 3 and 4) were always treated as fixed factors, whereas individual was treated as a random factor. Following the guidelines presented in Zar (1984), the *F*-test for individual effects was computed as the mean square (MS) individual divided by MS residual. In contrast, *F*-values of fixed factors (speed and marker) were computed as MS of the fixed effect divided by the two-way interaction term of the random and fixed effect. Both marker×speed and speed×individual two-way interaction terms were divided by the MS residual in order to determine the *F*-value. The two-way interaction term of the speed and marker factors was divided by the three-way interaction term (speed×marker×individual) to determine the *F*-value.

Separate two-way ANOVAs were performed on each of the displacement, time and velocity variables for each marker, and this procedure better clarified how speed affected the displacements for different portions of the pectoral fin edge. The *F*-value for speed effects was computed as MS speed divided by MS speed×individual. The two-way interaction term and the individual effect were tested over the residual in order to determine *F*-values.

Results

Movement patterns of the fin

Fig. 2 illustrates the three orthogonal displacements of the fin tip (marker 4) relative to points on the body of the fish (Fig. 1). The lateral (abduction–adduction), longitudinal (protraction–retraction) and vertical (levation–depression) displacements of the fin varied cyclically with time (Fig. 2). At the lowest swimming speed, the fin cycled through abduction and adduction with no interruption in lateral movement of the fin (Fig. 2A). However, at the highest swimming speed, the fin often remained against the body for as much as 25 % of a cycle (Fig. 2B), and we refer to this as the pause portion of the cycle. After the pause, the cycle repeated again, beginning with fin abduction. At the slowest swimming speed, the vertical, longitudinal and lateral movements all tended to have rather regular and smooth reversals of direction (Fig. 2A). In contrast, at the highest swimming speed, transitions in the direction of longitudinal and lateral movements were often less regular and occurred after periods of relative stasis (plateaux in Fig. 2B).

Regardless of the swimming speed, maximal abduction (maximum *z*) was nearly synchronous with maximal depression (minimum *y*) of the tip of the fin (Fig. 2). During much of fin abduction, the fin was simultaneously depressed (decreased *y*) and protracted (increased *x*). Similarly, during much of fin adduction simultaneous retraction and levation of the fin tip occurred. The greatest speeds (steepest slopes in Fig. 2) of fin adduction and retraction usually occurred midway between the times of maximal adduction and abduction.

Figs 3 and 4 illustrate one cycle of the longitudinal and vertical displacements of the fin edge relative to points on the body of the fish (Fig. 1) for the slowest and fastest swimming speeds. Hence, these plots are similar to a lateral view of the fish because its swimming speed precisely matched the flow speed. The arrows in Figs 3 and 4 indicate the direction of movement of each marker during the cycle.

At the slowest swimming speed (Fig. 3), all portions of the fin primarily moved

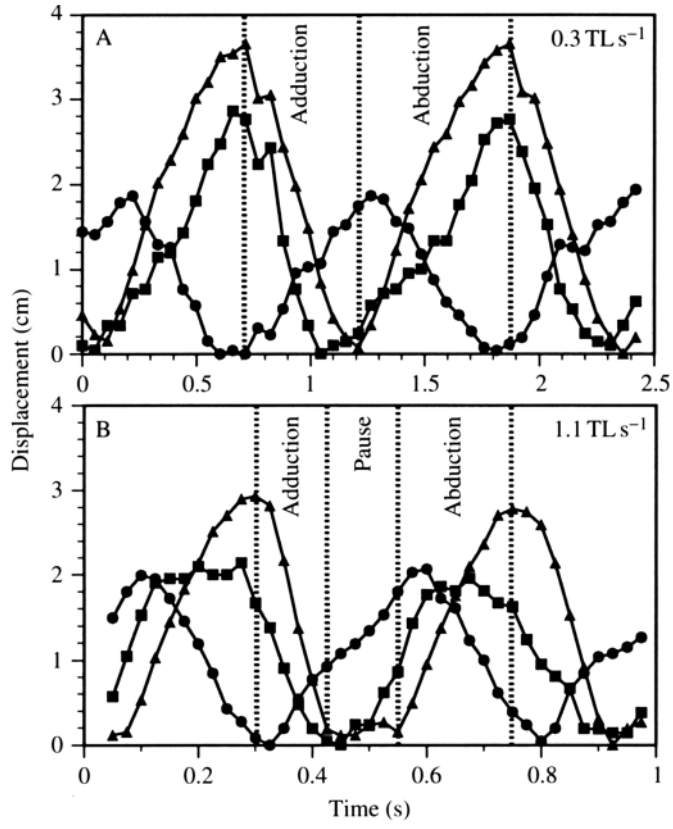

Fig. 2. Displacements of the most dorsal marker (marker 4) relative to the body for two fin beat cycles in one bluegill sunfish at (A) the slowest ($0.3\,TL\,s^{-1}$) and (B) the fastest ($1.1\,TL\,s^{-1}$) swimming speeds. The longitudinal (*x*) and vertical (*y*) displacements were calculated relative to the anterior base of the anal fin, whereas lateral (*z*) displacement was calculated relative to the base of the left pectoral fin. All values were also standardized by subtracting the minimal value observed over the illustrated time interval. Negative slopes for the curves of *x* (■), *z* (▲) and *y* (●) indicate fin retraction, adduction and depression, respectively.

anteriorly and ventrally and then posteriorly and dorsally. Hence, almost immediately after maximal protraction, the fin was also maximally depressed; it then returned to its original position by simultaneous retraction and levation. Because the paths traveled by markers 3 and 4 during protraction were dorsal to those traveled during retraction, these paths generally traced a 'counter-clockwise' loop when viewed laterally (Fig. 3). In contrast, the more ventral markers (1 and 2) generally traced paths with a 'clockwise' orientation (Fig. 3).

Overall fin movements at the highest swimming speed (Fig. 4) differed considerably from those at the lowest speed (Fig. 3). The dorsal portions (markers 4 and 3) of the fins generally traced more circular paths (in lateral view) compared with the paths traced at slower speeds. The major axis of the loops traced by the ventral markers (1 and 2) was oriented vertically (Fig. 4), whereas the loops during slower speeds had a more horizontal orientation (Fig. 3). At high speed (Fig. 4), all portions of the fin edge began moving with

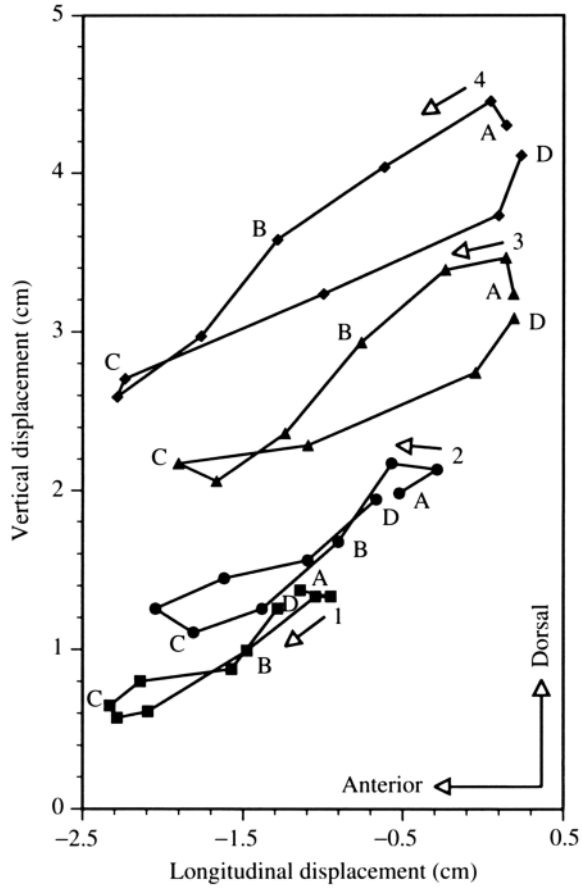

Fig. 3. Longitudinal (x) and vertical (y) displacements for all four fin markers relative to a point on the body of the fish during one fin beat cycle in one individual swimming at the slowest speed (0.3 TL s^{-1}). The reference point (x=0, y=0) on the body was the location of the attachment of the anterior base of the anal fin to the body. Although marker position was measured every 0.055 s during the fin beat cycle, only every other value from the data collected is shown for clarity. Arrows indicate the direction of movement of the markers during the fin beat. Homologous elapsed times for different markers are indicated by A (0 s), B (0.33 s), C (0.66 s) and D (0.99 s). ■, marker 1; ●, marker 2; ▲, marker 3; ◆, marker 4.

simultaneous protraction and levation, and then, after maximal levation, the markers were depressed with only a small amount of simultaneous protraction. Following maximal protraction, the fin edge briefly underwent simultaneous retraction and depression. After maximal depression, simultaneous retraction and levation brought the fin edge against the body. Finally, a small amount of levation and protraction occurred as the fin remained near the body during the pause in preparation for the next fin abduction.

Effects of speed

In addition to the changes with speed mentioned in the above description of fin movements, we quantitatively compared seven kinematic variables (based on the

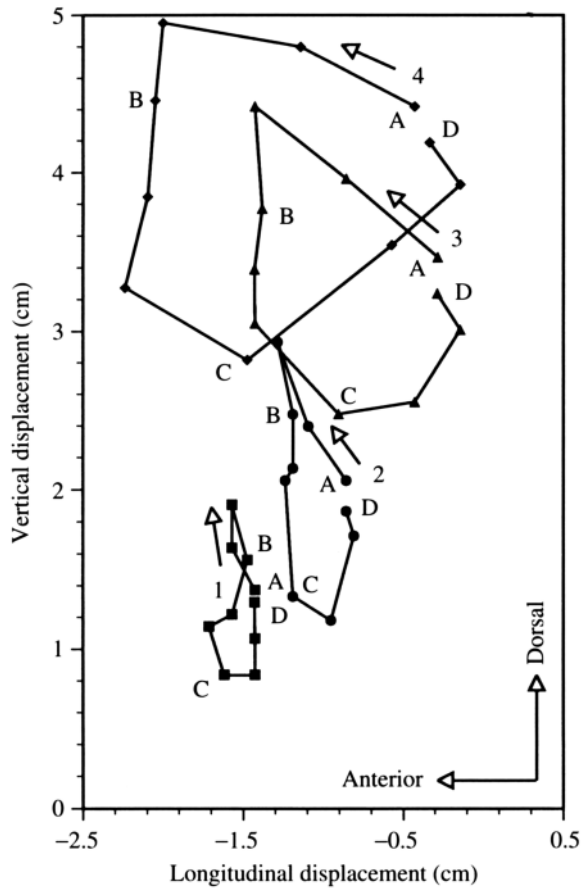

Fig. 4. Longitudinal (*x*) and vertical (*y*) displacements for all four fin markers relative to a point on the body of the fish during one fin beat cycle of swimming at the fastest speed (1.1 TL s^{-1}). The individual, calculations and labeling are the same as in Fig. 3. Although marker position was measured every 0.025 s during the fin beat cycle, only every other value from the data collected is shown for clarity. Homologous elapsed times for different markers are indicated by A (0 s), B (0.15 s), C (0.30 s) and D (0.45 s).

movements of marker 4) among the five different speeds (Table 2). The most conspicuous change with speed occurred for the fin beat frequency (Fig. 5, Table 2), which approximately doubled (from 1.2 to 2.1 Hz) as the swimming speed increased from 0.3 to 1.0 TL s^{-1}. Frequency did not increase significantly between 1.0 to 1.1 TL s^{-1}, but the bluegill often began to use axial and caudal fin locomotion in addition to pectoral fin locomotion at 1.1 TL s^{-1}. This change in gait corresponds to that described in unpublished work by P. W. Webb on *Lepomis macrochirus* and cited in a recent review by Alexander (1989).

Five out of the six variables measuring maximal velocity of the fin tip (marker 4) changed significantly with increased swimming speed (Table 2), and Fig. 6A,B shows the changes associated with swimming speed during both abduction and adduction. Maximum fin velocity increased significantly with swimming speed during abduction in

Table 2. *Summary of* F*-tests for significance of effects in separate two-way ANOVAs performed on each kinematic timing and velocity variable*

	Effect		
Variable	Speed (4,12)	Individual (3,60)	Speed×Individual (12,60)
ABDMINX	14.7***	12.9***	2.7**
ABDMINY	14.5***	7.1***	3.3***
ABDMINZ	21.8***	17.1***	1.9*
ADDMAXX	2.3	28.1***	1.7
ADDMAXY	7.3**	4.2***	3.9***
ADDMAXZ	18.9***	8.0***	2.0*
FREQ	28.2***	36.1***	6.8***

Degrees of freedom are given under each effect.
*P<0.05; **P<0.01; ***P<0.001.
Abbreviations for variables in this and other tables are explained in the text.

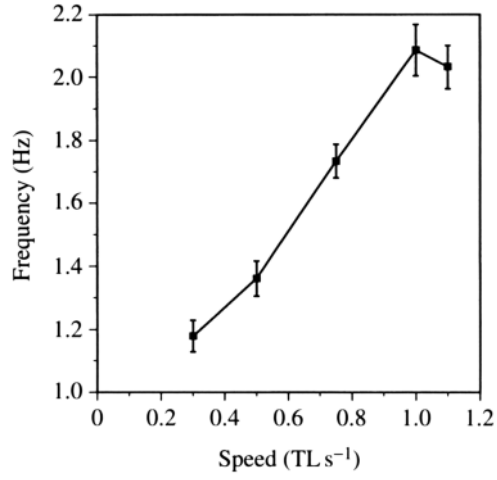

Fig. 5. Frequency of fin beats increased with an increase in the swimming speed in *Lepomis macrochirus*. Points are the mean values ± 1 S.E.M. (N=16) for all individuals at a given swimming speed.

all dimensions (Fig. 6A) and during adduction in all dimensions except for fin movement in the longitudinal dimension (Fig. 6B). High inter-individual variation (Table 2, Individual) in some variables decreased the likelihood of detecting significant changes with speed.

At the lowest swimming speed, the time taken to reach maximal lateral displacement increased from dorsal to ventral along the fin edge (Fig. 7A), resulting in phase lags between markers 4 and 3, 4 and 2, and 4 and 1 of 12 °, 18 ° and 32 °, respectively, all of which were significantly different from zero. In contrast, with only one exception (a phase lag of −13 ° found between markers 4 and 1 at the highest swimming speed), at all

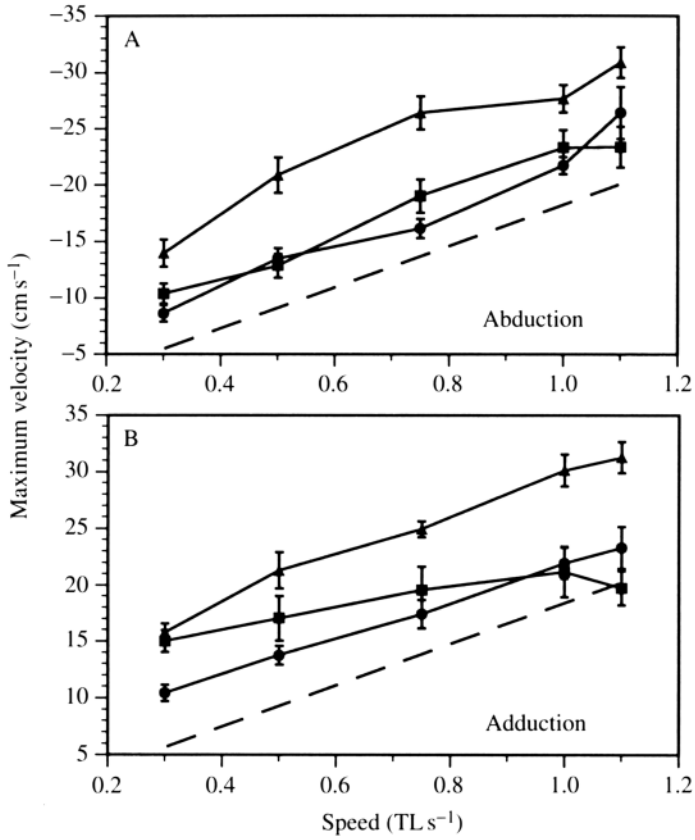

Fig. 6. Maximal velocities of the tip of the fin relative to the body in all dimensions during the abduction (A) and adduction (B) portions of the fin beat cycle. The mean values ± 1 S.E.M. for all individuals at each swimming speed are plotted (Table 2 summarizes significant change with speed). Values during abduction are given as negative velocities because the fin is moving in the opposite direction compared with adduction. Longitudinal (*x*), vertical (*y*) and lateral (*z*) velocities are indicated by ■, ● and ▲, respectively. (A) Velocities in the *x*, *y* and *z* dimensions represent protraction, depression and abduction speeds of the fin tip, respectively. (B) Velocities in the *x*, *y* and *z* dimensions represent retraction, levation and adduction speeds of the fin tip, respectively. The dashed line represents the mean speed of movement (in cm s^{-1}) for the fish used in this study.

other swimming speeds there was no significant phase lag between the maximal lateral displacement of marker 4 and that of the more ventral markers (Fig. 7B).

To clarify the extent of differences in amplitudes of movement within the fin edge, we performed three-way ANOVAs which revealed that fin excursions in all three dimensions (XEX, YEX and ZEX) varied significantly among different positions (Table 3, Marker). Within each speed, the amplitudes of movement increased from ventral to dorsal along the distal edge of the fin (Fig. 8). Longitudinal and lateral excursion during the fin beat cycle also varied significantly with speed (Table 3, speed).

We used separate two-way ANOVAs (Table 4) for each excursion of each marker to

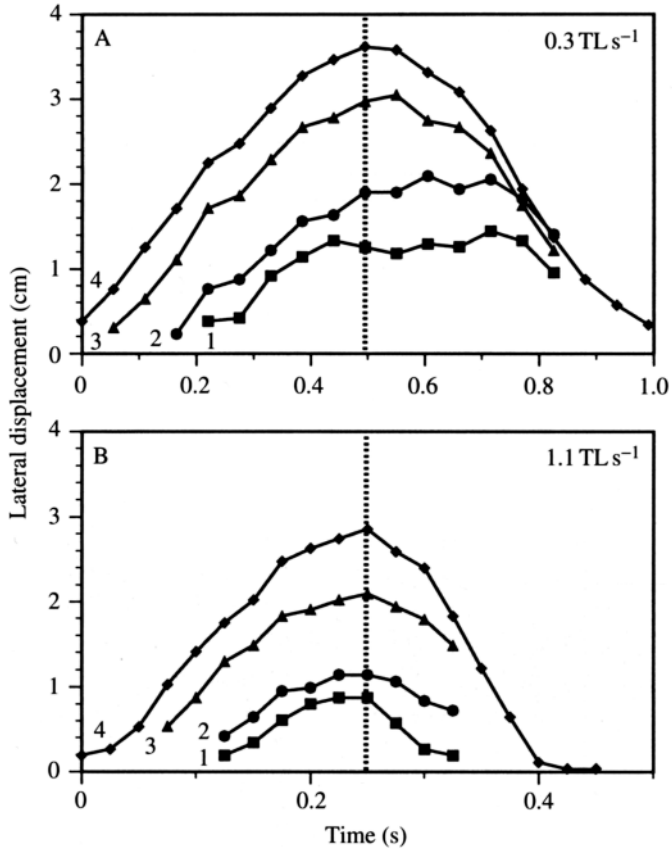

Fig. 7. Lateral displacement (z) relative to the body for all four fin markers during one fin beat cycle at the lowest (A) and highest (B) swimming speeds. From dorsal to ventral the markers are represented by ◆, ▲, ● and ■, respectively. Increased values of z indicate greater distance from the body (adduction). Some values are missing because not all markers were clearly visible in ventral view for the entire cycle. (A) At the lowest speed ($0.3\,TL\,s^{-1}$), the times of maximum lateral displacement occurred successively later from dorsal to ventral along the distal edge of the fin. (B) At the highest swimming speed ($1.1\,TL\,s^{-1}$), all four markers reached their maxima at the same moment. The vertical line marks the maximal lateral displacement of marker 4.

clarify whether all amplitudes of movement were universally affected by changes in swimming speed. The clearest effect of speed was on the amplitude of the lateral movements for the three most ventral fin positions (1ZEX, 2ZEX and 3ZEX). Three additional excursions (2XEX, 3YEX and 4XEX) varied significantly with speed, but the highly significant interaction terms somewhat complicate the interpretation of these results. Consequently, we examined the mean values for the excursions in all three dimensions (Fig. 8) to determine whether there were some consistent trends with speed. When significant changes did occur for the amplitude of longitudinal and lateral movements (Fig. 8A,C), these quantities generally declined with increasing speed (although marker 4 shows no relationship between swimming speed and lateral

Table 3. *Summary of* F*-tests for significance of effects in separate three-way ANOVAs performed on each kinematic displacement variable*

	Effect						
Variable	Speed (4,12)	Marker (3,9)	Individual (3,240)	Speed× Marker (12,36)	Speed× Individual (12,240)	Marker× Individual (9,240)	Speed× Marker× Individual (36,240)
XEX	4.5*	57.6***	295.1***	0.8	16.2***	18.5***	2.8***
YEX	3.0	60.0***	151.3***	1.3	24.3***	12.1***	5.1***
ZEX	4.8*	159.3***	720.6***	6.3***	33.8***	35.4***	2.1***

Degrees of freedom are given under each effect.
*P<0.05; **P<0.01; ***P<0.001.

displacement). In contrast, the only significant change in amplitude of vertical movements involved increased values with increased speed, and such a trend was more apparent for the dorsal half of the fin than for the ventral half (Fig. 8B).

Angle of attack

All of the results described so far concern movements of the fin relative to a frame of reference within the fish, and this information is needed to understand anatomical function. However, the movements of the fin relative to the fluid must be examined when considering the mechanisms of propulsion. Fig. 9 illustrates the movement of the fin markers with respect to a fixed frame of reference; the paths shown correct for the speed of the flow tank and would correspond to a lateral view of the fish if it were swimming in still water. A conspicuous feature of the slow ($0.3\,TL\,s^{-1}$) swimming speed was that the speed of the fin tip during mid-retraction (movement in the longitudinal dimension) exceeded the swimming speed of the fish. Therefore, the fin had backward 'slip' through the water. The extent of this backward slip diminished as the swimming speed increased, as indicated by the decreased values of mean (N=16) maximal retraction speed divided by swimming speed (2.75, 1.90, 1.45, 1.18, 1.00). Within a single speed, the dorsal portions of the fin could slip while effectively no slip occurred for more ventral portions of the fin (Fig. 9A).

The trajectory (Fig. 9 dotted lines) of an object through a fluid determines the incident flow, which is required to calculate the angle of attack. For plate-like (planar) objects, one must also determine the orientation of the plane relative to the incident flow. We determined the equations of planes containing two distal points (markers) and one point at the base of the fin; these three points defined the planar fin element. We determined the orientation of these planar fin elements by finding the line of intersection between the planar fin element and a parasagittal (x–y) plane (lateral view) and then calculating the angle between this line and the x axis (equal to the overall direction of travel). Because fin movements were bilateral, it seems likely that the lateral movements would generate opposing lateral forces, which would cancel each other out. The orientation of the fin occasionally precluded measuring the z coordinate which, in turn, precluded performing

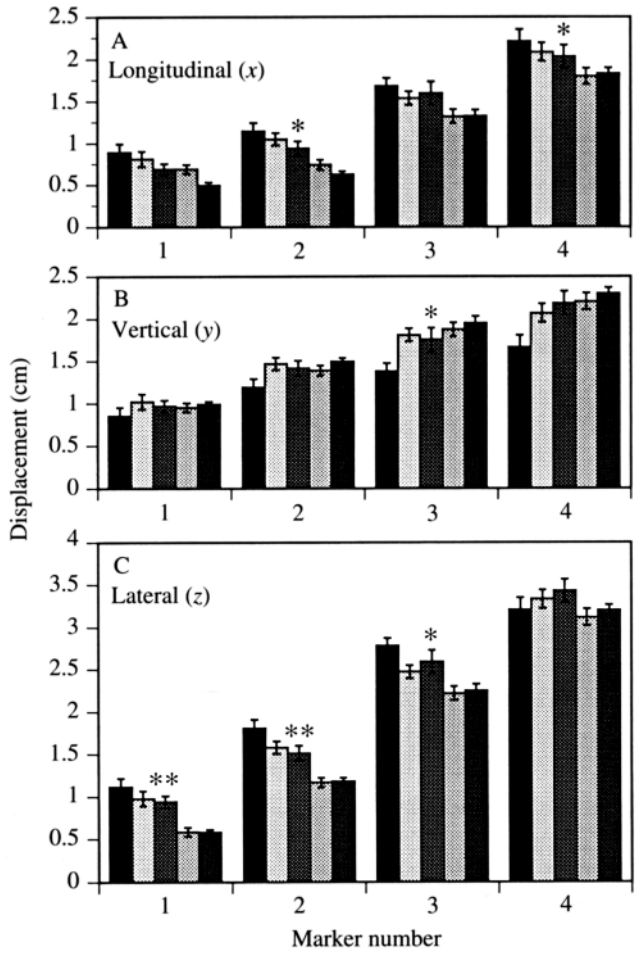

Fig. 8. Summary of the mean excursions (amplitudes) measured for the four markers relative to the body of the fish for three dimensions at five speeds. Means ± 1 S.E.M. (N=16) for all individuals at the five swimming speeds are shown. Speed increases from left to right for each marker. Marker excursions significantly affected by swimming speed (ANOVA, Table 2) are indicated by *P<0.05 and **P<0.01. (A) Longitudinal (x) excursion (protraction–retraction); (B) vertical (y) excursion (depression–levation); (C) lateral (z) excursion (abduction–adduction).

these three-dimensional calculations for some portions of the fin beat cycle. It should be emphasized that these calculations generate a 'geometrical' angle of attack that reflects the angle of the fin element to the parasagittal plane and not the true angle of the fin element with respect to the flow itself.

The upper part of Fig. 10 illustrates the orientations of such planar fin elements as they intersect the parasagittal plane. Table 5 indicates the discrepancies between the angles of attack (α) that would result from using only a two-dimensional lateral view of the fish and the angle of attack calculated using a three-dimensional analysis. During early abduction (and depression) of the fin tip (approximately 0–16 % of the cycle, Table 5), the dorsal

Table 4. *Summary of* F*-tests for significance of effects in separate two-way ANOVAs performed on each kinematic displacement variable for each marker*

	Effect		
Variable	Speed (4,12)	Individual (3,60)	Speed×Individual (12,60)
1XEX	1.8	42.1***	9.7***
1YEX	1.0	29.1***	5.9***
1ZEX	7.1**	302.0***	12.2***
2XEX	4.9*	63.7***	7.6***
2YEX	2.1	35.3***	8.7***
2ZEX	9.0**	101.0***	6.5***
3XEX	3.0	99.0***	5.2***
3YEX	3.3*	37.9***	7.5***
3ZEX	5.3*	147.0***	10.8***
4XEX	3.8*	122.0***	3.9***
4YEX	2.1	64.8***	13.7***
4ZEX	1.1	328.0***	12.3***

Degrees of freedom are given under each effect.
*P<0.05; **P<0.01; ***P<0.001.

planar fin element was nearly parallel to its trajectory or had small negative values of α. With continued fin abduction (approximately 25–40 % of the cycle, Table 5), α of the planar fin elements approximated 40–50 °. During fin depression and abduction (Table 5), the orientation of the planar fin elements at 1.1 TL s^{-1} was more nearly parallel to the overall direction of the travel of the fish than at the slow speed (Fig. 10; Table 5, planar angle). During early levation (and retraction) of the fin at the slowest speed, α of the planar element was large and positive. The large differences shown in Table 5 reveal that the two-dimensional approximations are particularly inaccurate during early fin abduction.

Discussion

Overall fin movement pattern

For hydromechanical modeling it is convenient to consider the pectoral fins as a rigid plate. However, our observations of *Lepomis*, combined with previous studies of pectoral fin swimming (Webb, 1973; Geerlink, 1983), emphasize that the highly compliant pectoral fins differ considerably from a rigid plate. For *Lepomis*, there are five lines of evidence supporting this conclusion. First, the amplitude of movement in each dimension is different for the four marked portions of the fin. Second, as illustrated in Fig. 3, at some swimming speeds the ventral portions of the fin 'loop' in a different direction from the dorsal portions of the fin (as transcribed by marker movements in lateral view). Third, at some speeds, phase lags occur between the maximum lateral displacement of marker 4 (the most dorsal and distal marker) and the maximum lateral displacement of the rest of the fin. Fourth, angles of attack calculated for the dorsal and ventral portions of the fin are

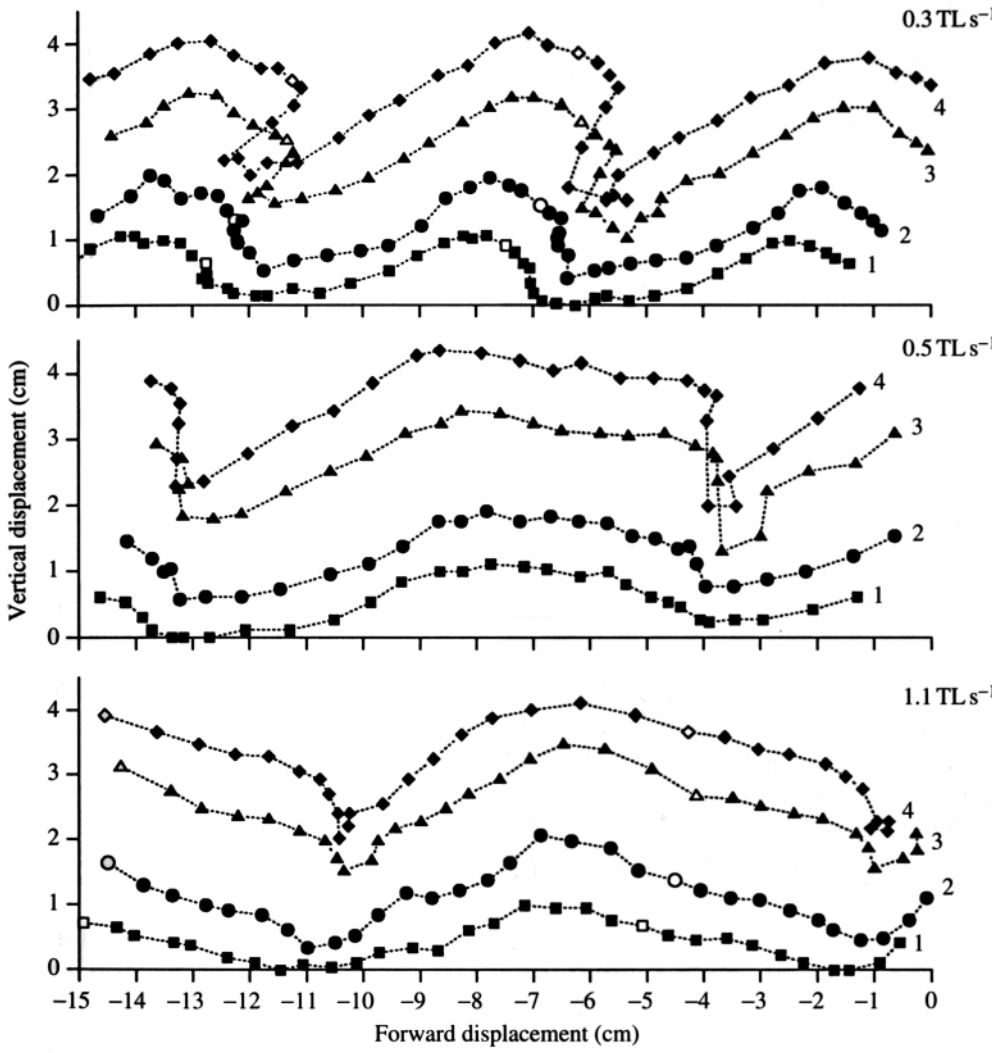

Fig. 9. Lateral view (from a fixed frame of reference) of the paths (dotted lines) traveled by the four markers on the distal edge of the fin for a single individual. The fish is traveling from right to left, and the *x* and *y* axes are drawn to the same scale so that the view is not distorted. The intervals between successive points are 0.055, 0.055 and 0.025 s respectively, for the slowest to the fastest speed. Two fin beats are shown for the slowest swimming speed (0.3 TL s^{-1}), whereas slightly more than one is given for the higher speeds. In this figure, all displacements have been standardized so that the most ventral displacement of the most ventral marker equals zero. The open symbols bracket the time intervals used for showing the movements of the markers relative to the body of the fish (Figs 3 and 4). Note that the changing spacing between points reflects changes in marker velocity.

quite different. Fifth, when the swimming speed of the fish changes, there are many correlated changes in kinematic variables.

When considering how kinematic variables varied among markers, it is useful to consider how marker placement alone could affect any of these quantities. If all marked

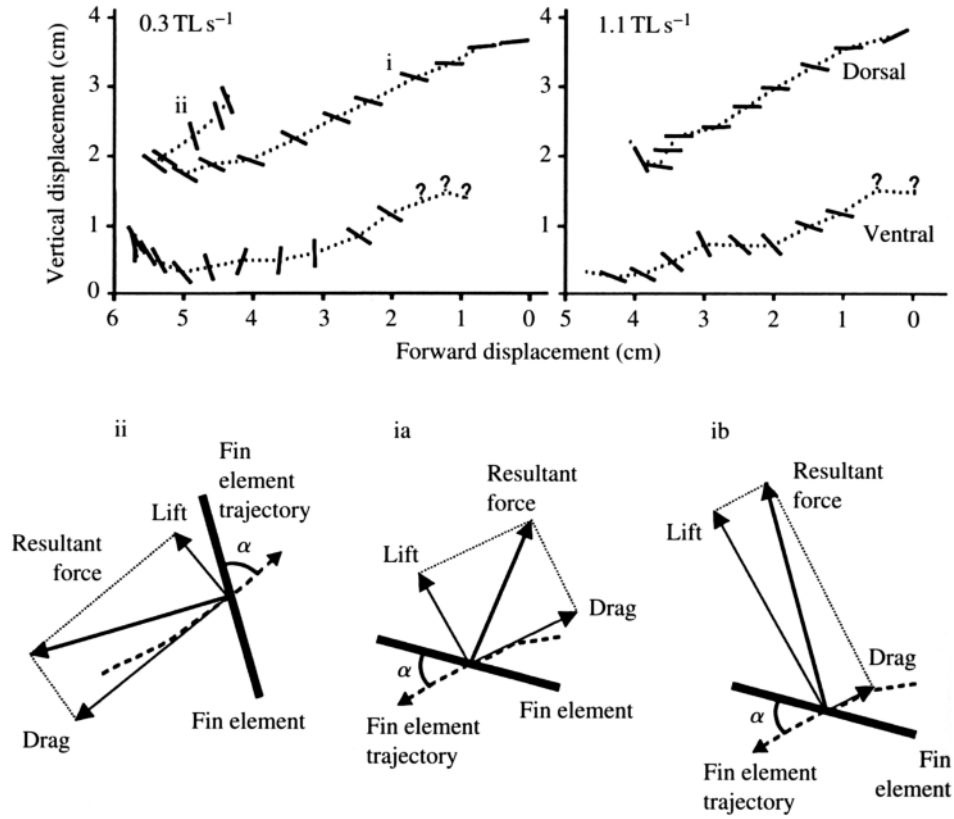

Fig. 10. Lateral view (from a fixed frame of reference) of the path (dotted line) and orientation (short dark lines) of the dorsal and ventral planar fin elements for a portion of one fin beat cycle. The paths shown are for the midpoint between the two fin edge markers. The dorsal fin element was defined by markers 4 and 3 and the basal location of the most dorsal fin ray. The ventral element was defined by markers 2 and 1 and the basal location of the most ventral fin ray. The *x* and *y* axes are scaled and oriented as in Fig. 9. For successive images, the time increments for the slow and fast speeds are 0.055 and 0.025 s, respectively. The short thick lines indicate the orientation of the line formed by the intersection of the *x*–*y* plane and the plane containing the fin element. ? indicates values missing due to a lack of the lateral coordinates. Insets ia, ib and ii represent hypothetical vector diagrams for the portions of the fin beat cycle labeled i and ii. For these insets, the orientation of the vectors is based on experimentally observed data (same individual as in Figs 2, 3, 4 and 10), but the magnitudes of the force vectors are hypothetical. See Table 5 and text for further explanation.

fin rays had identical rotational movements in all three dimensions, then the amplitude of linear displacement of each marker would be proportional to fin ray length. The average lengths of the marked fin rays (Table 1) increased more than twofold from the most ventral to the most dorsal markers (1–4) with values of 1.9, 2.7, 3.6 and 4.2 cm, respectively. Thus, if linear displacement (Fig. 8) divided by fin ray length is a constant, then the kinematic variation observed among markers could be a simple consequence of morphological variation. Interestingly, the highly significant among-marker variation in the amplitude of vertical displacement (Table 3, YEX) appears to conform closely to this

Table 5. *Calculation of the angle of attack for two sample fin elements using both two- and three-dimensional data*

Time		Dorsal fin elements (markers 4 and 3)					Ventral fin elements (markers 2 and 1)				
Begin	End	Path angle	Planar angle	Planar α	2-dim angle	2-dim α	Path angle	Planar angle	Planar α	2-dim angle	2-dim α
Slow (0.3 TL s^{-1})											
5 %	10 %	–9	–6	3	85	86	18	–	–	–51	–69
25 %	30 %	–25	15	40	51	76	–21	33	54	–50	–29
40 %	45 %	–6	18	24	32	38	–11	–70	–59	–39	–28
65 %	70 %	139	74	65	–84	43	86	78	–8	–51	–55
Fast (1.1 TL s^{-1})											
11 %	16 %	–15	–26	–11	43	58	6	–	–	–75	–81
26 %	32 %	–33	3	36	41	74	–24	19	43	–66	–90
42 %	47 %	–48	–1	49	16	64	–29	63	–88	–62	89
58 %	63 %	61	60	–1	84	23	–10	21	31	–31	–21

The first two columns (Time: begin, end) indicate the interval (in percentage of the fin beat cycle) between successive images used for calculations within each row (0 and 100 % represent the times of minimal lateral displacement of marker 4).

All other table entries are angles (in degrees).

Path angle is the orientation of the trajectories (dotted lines) shown in Fig. 10.

Planar angle is the angle between the line of intersection between the fin element plane and the *x*–*y* plane, and the *x* axis.

2-dim angle is the angle between the line segment connecting the *x* and *y* coordinates of the two fin edge markers and the *x* axis.

α indicates the angle of attack estimated from either the planar angles (based on three-dimensional data: planar α) or two-dimensional calculations (2-dim α).

All calculations are based on the data shown in Fig. 10.

expectation based on fin ray length. For example, at 1.1 TL s^{-1}, the *y* excursions (Fig. 8B) divided by fin ray length for markers 1–4 were 0.51, 0.56, 0.54 and 0.55, respectively. At other speeds, these relative vertical excursions had similarly small variation among markers, with no clear pattern of change from the most ventral to the most dorsal positions. Consequently, the fin rays appear to undergo similar amounts of vertical rotation about their basal points of attachment. In contrast, the relative amplitudes of lateral (0.30, 0.44, 0.62 and 0.76 ray lengths) and longitudinal (0.26, 0.23, 0.36 and 0.44 ray lengths) displacement showed an approximately twofold increase from the most ventral to the most dorsal marker positions. Therefore, the highly significant among-marker variation in lateral and longitudinal movement resulted from both variable fin ray length and proportionately greater amounts of rotation for the more dorsal fin rays in these two directions.

Several additional aspects of among-marker variation in kinematics cannot be explained simply by variation in fin ray length. Loops traced by different markers in lateral view varied both in their direction (Fig. 3, clockwise *versus* counterclockwise) and shape (Fig. 4, proportionately more vertical displacement of ventral positions). For the slowest speed, different portions of the fin edge also had highly significant phase lags in the times to maximal displacement. The angles of attack varied considerably between the ventral and dorsal planar fin elements (Fig. 10). Changes in kinematics associated with speed also varied among markers. For example, the lateral displacement of the three most ventral markers decreased significantly with increased speed, whereas that of the most dorsal marker did not (Fig. 8C). Therefore, the vast majority of kinematic variables which we quantified had at least some variation that was associated with fin ray position but could not be attributed simply to fin ray length.

Our kinematic data support the idea that the dorsal portion (first two fin rays) of the fin often acts as a ‘leading edge’ as suggested by previous studies (Webb, 1973; Geerlink, 1983). All significant differences in the timing of kinematic events of marker 4 *versus* other markers occurred as a result of more ventral markers lagging behind the movements of marker 4. The ventral portion of the fin often lagged behind the dorsal portion of the fin during both protraction and retraction. For example, during early abduction and protraction, movement of the fin can be grossly visualized as peeling a triangular piece of tape off a surface by grasping the corner corresponding to the dorsal and distal tip of the fin. Perhaps this leading motion of the dorsal pectoral fin ray helps to minimize suction between the fin and the body during early abduction.

The extent to which pectoral fin movements are generated actively (by muscle) *versus* passively (by resistive forces) is an interesting area for future work. The observation that the fin is retracted faster than the forward swimming speed of the fish indicates that some muscular effort must be involved in this stage of the fin movements, but it is possible that slower retraction movements could result from the water pressing the fin back towards the body. The lags in movement of successively more ventral rays are generally consistent with those that could be generated passively by moving a rod with an attached piece of cloth through fluid. The most dorsal supporting element of the pectoral fin of most teleost fishes is a specialized splint-like ray that is firmly attached to the first fin ray (Gosline, 1980). The muscles inserting onto this complex structure are distinct from the fin

adductors and abductors that attach to more ventral fin rays (Winterbottom, 1974). Therefore, it seems anatomically feasible that activity of these muscles could move the entire fin as long as the fin membrane is taut. Electromyographic studies presently under way will help to resolve these issues.

The effects of speed

Changes in fin beat frequency showed the clearest association with increased speed (Table 2, Fig. 5). Dividing swimming speed by fin beat frequency provides an estimate of the distance traveled per cycle. From the slowest to the fastest swimming speeds observed for the bluegill these quantities were 4.5, 6.4, 7.9, 8.5 and 9.9 cm cycle^{-1}, respectively. These results are analogous to the increase in stride length that commonly occurs for limbed animals. The observation that swimming speed increased more rapidly than fin beat frequency suggests that factors besides fin beat frequency must contribute to increased swimming speed. The bluegill also had considerable variations in the amplitude, direction and speed of fin edge movements that were associated with increased swimming speed.

Because the dorsal margin of the fin generally acted as a leading edge, accounting for its orientation helps to explain some of the variation that was associated with speed. Assuming that the leading edge is a straight line between marker 4 and a point at the base of the most dorsal fin ray, it is possible to estimate the angle of this line segment as seen from its projection in lateral (x–*y* plane), ventral (*x*–*z* plane) and anterior (*y*–*z* plane) views. For example, at 0.3 TL s^{-1}, when the fin tip was maximally levated (1.5–1.8 cm above the fin base), the leading edge was oriented dorso-caudally at an angle of about 28° with respect to the horizontal, whereas at 1.1 TL s^{-1}, this angle approximated 48° (tip 2.6–2.8 cm above base). At maximal depression of the fin tip at 0.3 TL s^{-1}, the tip of the fin was at a height approximately equal to that of the fin base, resulting in an orientation of approximately 90° with respect to the vertical when viewed anteriorly. At 1.1 TL s^{-1}, the maximally depressed tip of the fin was only slightly (0.3–0.5 cm) above the base of the fin, resulting in an angle of about 80° relative to the vertical in the *y*–*z* plane. Therefore, the trend in increased vertical movement with increased speed (Fig. 8B) was primarily the result of increased dorsal movement of the fin during levation, rather than a change in the most ventral position at maximal depression.

At all swimming speeds for the bluegill, the tip of the leading edge was always posterior to its base, resulting in acute angles between it and the longitudinal axis of the fish as seen in a ventral view of maximal fin protraction (*x*–*z* plane). At 0.3 and 1.1 TL s^{-1}, these angles were approximately 62° and 55°, respectively. Webb (1973) found that these angles were also acute for the surf perch but, in contrast to the bluegill, they increased from 62 to 88° as swimming speed increased from 0.5 to 3.6 TL s^{-1}. For the labrid *Coris formosa*, these angles show a broad range of variation from approximately 70 to 120°, but swimming speed was not systematically controlled in this study (Geerlink, 1983).

The magnitude of the velocity of the tip of the fin ray depends on the speed at which the fin muscles rotate the base of the ray as well as on the length and orientation of the fin ray. If a fin ray perpendicular to the body were rotated posteriorly within the horizontal (*x*–*z*)

plane at a constant angular velocity, then the speed of adduction (*z* direction) would be proportional to the cosine of the angle between the ray and the longitudinal axis of the fish. In contrast, the retraction (*x* direction) speed would be proportional to the sine of the same angle. Hence, in this hypothetical case, adduction speed is maximized when the fin is nearly parallel to the body, whereas retraction speed is maximized when the ray is nearly perpendicular to the body. In the bluegill, the angle between the leading edge of the fin and the longitudinal axis (in the *x*–*z* plane) was always considerably less than 90 °. Because the maximal adduction speed (Fig. 2, slope of *z*) of the bluegill fin tip consistently occurred midway through adduction, this pattern of velocity cannot be explained as being the simple result of the angular orientation (in the *x*–*z* plane) of the leading edge. Instead, the speed of adduction is the result of rotation of the leading edge in both the *x*–*z* and the *y*–*z* planes with component angular velocities that are not constant through time.

At the highest swimming speed, the pectoral fin of the bluegill remained near the body for as much as 25 % of a cycle after adduction (Fig. 2B). This pause in fin movement made it difficult to evaluate the proportion of time that the fin spent in each phase of the fin beat cycle. During the pause, the fin orientation was unsuitable for producing thrust; thus, decreasing the amount of time spent in this 'pause' or 'refractory' period is a potential mechanism for meeting the requirements of increased thrust for increased swimming speed. Surprisingly, in bluegill, the pause only appeared at the highest swimming speeds and a regular pause phase was not apparent at lower speeds. In contrast, as the swimming speed of the surf perch increased from 0.5 to 4.4 TL s^{-1}, Webb (1973) found that the refractory portion of the pectoral fin beat cycle decreased from approximately 65 to 0 %. This difference in fin movements may contribute to the ability of the surf perch to use pectoral fin locomotion over a larger range of speeds than can the bluegill.

When considering thrust production, the retraction movements are also particularly important because of their orientation parallel to the overall direction of travel. Within the fin beat cycle, the timing of maximal retraction speed was more variable than that of adduction. The maximal speed of retraction usually exceeded the swimming speed, resulting in a backward slip of the fin with respect to the water. Similarly, for aquatic undulatory swimming, the speed of posterior wave propagation exceeds the swimming speed and comparisons of the wave and swimming speeds are often used as indices of efficiency (Gray, 1968). For the bluegill fin tip, the ratio of maximal retraction speed to swimming speed declined from 2.75 to 1.00 as speed increased. Thus, either the efficiency of pectoral fin locomotion increases with increased speed or, more probably, different mechanisms of propulsion contribute to thrust as speed increases.

Lift- versus *drag-based locomotion*

Pectoral fin swimmers have been considered as using either lift- or drag-based propulsive mechanisms (Blake, 1983; Webb and Blake, 1985). We feel that the difficulties both in quantifying the relevant flow and in integrating forces over the entire fin make quantitative estimates of the lift and drag forces in the bluegill extremely difficult. However, we discuss some of our kinematic observations of bluegill, which are at least consistent or inconsistent with the alternative mechanisms that have been proposed for pectoral fin swimming.

For drag-based swimming, one would expect pectoral fin rotation primarily in the horizontal plane, with the fin surface perpendicular to the overall direction of travel (Webb and Blake, 1985). In contrast, for lift-based swimming, one would expect a vertical upstroke of the fin, with the anterior fin edge dorsal to the posterior trailing edge followed by a downstroke with a reversed orientation of the anterior and posterior edges of the fin. The intermediate pectoral fin kinematics of the bluegill sunfish (Figs 3, 4, 9 and 10) indicates that a complicated combination of these mechanisms produces thrust.

Purely drag-based locomotion should have very distinct propulsive and recovery phases (Webb and Blake, 1985). If the pectoral fins were retracted in a manner similar to the oars of a rowing boat, then the forward speed of the fish during the propulsive phase (retraction) should exceed that of the recovery phase (protraction). Hence, the swimming speed (*x* direction) would vary periodically and be in phase with fin retraction. Plots of the *x* displacement of the body of bluegill *versus* time (Fig. 11B) revealed no clear pattern of periodic variation associated with the fin beat cycle for any of the five swimming speeds. For drag-based propulsion, one would also expect 'feathering' of the fin during the recovery stroke. During fin depression and protraction, the orientation of the surface of the dorsal fin element was usually more nearly parallel to the overall trajectory than it was during retraction (Fig. 10), and this resembles the expectation of feathering a paddle.

When a flat plate (paddle) moves with constant speed through a fluid and its surface is perpendicular to the direction of movement, the thrust forces produced by drag on such a paddle are proportional to $(u-V)^2$, where u is the speed of the paddle relative to the object being propelled and V is the overall swimming speed. This relationship is the basis for a variety of drag-based models of propulsion by oscillating structures (Webb and Blake, 1985: equation 7-10). For the bluegill pectoral fin, $u-V$ is maximized at the maximal speeds of retraction. For swimming speeds of 0.3, 0.5, 0.75, 1.0 and 1.1 TL s^{-1}, mean maximal speeds of retraction minus V were 9.5, 8.1, 6.1, 3.3 and 0 cm s^{-1}, respectively. Despite the fact that maximal retraction speed usually exceeded swimming speed, $u-V$ was greater than zero for only a small portion of the fin beat cycle and for only the dorsal portions of the distal edge of the fin. In Fig. 9, when $u-V>0$, there is a brief reversal of direction, and for marker 4 at 0.3 TL s^{-1} this occurred for about 0.17 s, which was only 17 % of a cycle. These observations suggest that drag-based mechanisms of propulsion may not be sufficient to account for movement during the entire locomotor cycle.

One expectation for lift-based oscillatory swimming [such as the underwater 'flying' of penguins (Clark and Bemis, 1979)] is that the body should oscillate vertically. Webb (1973) did observe this for the pectoral fin swimming of the surf perch. In contrast, the vertical displacement of the body of the bluegill showed no conspicuous periodic variation at any of the swimming speeds (Fig. 11C). A lift-based mechanism of propulsion with varying orientations of the lift and drag forces acting on the pectoral fins could produce relatively constant forward speed and a lack of vertical oscillation.

Frictional drag forces are parallel whereas lift forces are perpendicular to the incident flow of fluid on an object. For the sake of simplicity, the incident flow on an object is often assumed to have an equal magnitude to, and an opposite direction from, the velocity of movement of an object. In Fig. 10 we used these assumptions combined with our experimentally observed trajectories and orientations of planar fin elements to consider

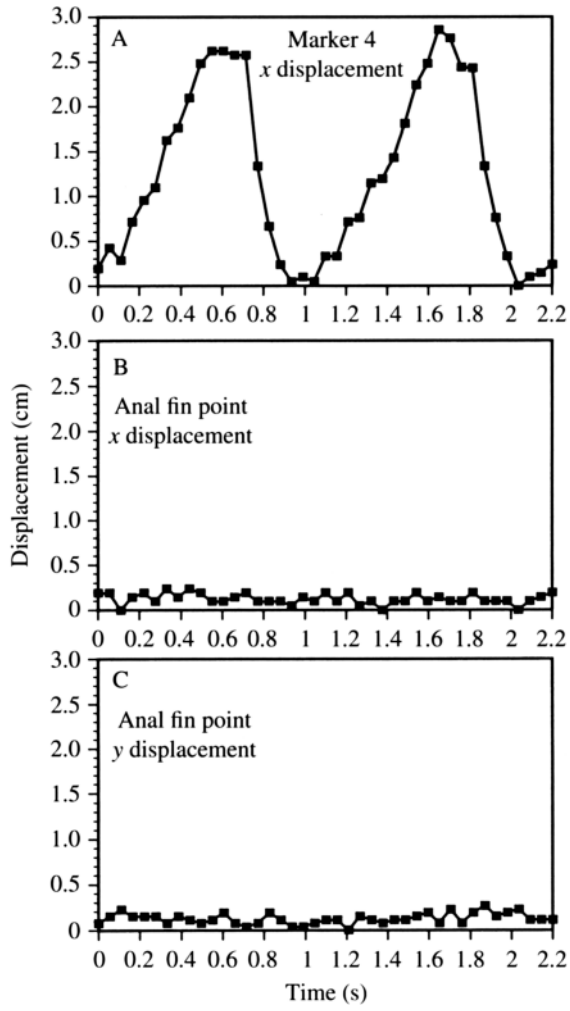

Fig. 11. Displacement of marker 4 and a body reference point over two fin beat cycles for one individual. (A) Longitudinal displacement of marker 4; (B) longitudinal displacement of a point marking the anterior point of the anal fin of the fish; (C) vertical displacement of the same reference point as in B on the body. Note that all graphs have been plotted to the same scale to emphasize that changes in the longitudinal and lateral positions of the reference point are small and show no pattern.

possible mechanisms of forward movement. The resultant force acting on the fin is the vector sum of the total lift and drag forces, and this vector must have a forward-directed x component in order to contribute to forward propulsion.

In some cases, it is possible to predict that the resultant vector has a forward-directed component. For these instances, the relative contributions of lift and drag can be estimated after the angle of attack has been determined (although the magnitudes of the lift and drag vectors may not be known). For example (Fig. 10, inset ii), if the trajectory of the fin element is oriented posteriorly, and α plus the acute angle between the fin

element and the horizontal exceeds 90°, then the drag forces acting on the fin will be much greater than the lift forces, and the resultant vector will always be oriented forward. In contrast, if the fin element has a forward trajectory (Fig. 10, insets ia and ib), then there will be a forward-directed resultant vector only if the sum of the *x* components of the drag and lift vectors is directed forward. Hence, the existence of a forward-directed resultant vector during most of pectoral fin depression (Fig. 10) can only be determined if the magnitudes of the lift and drag vectors are known precisely. The absence of noticeable deceleration (of the body) during fin depression and protraction suggests that the magnitude of the lift force may be sufficient to cause a forward-directed resultant vector. The orientations and trajectories of the fin elements also bear a striking resemblance to the orientation and movement path of certain insect wings during flight (Nachtigall, 1966), adding to the plausibility of a partially lift-based mechanism of pectoral fin locomotion.

Acceleration reaction force

In addition to lift- and drag-based forces, the acceleration reaction is a potential source of thrust force. In fact, the acceleration reaction may produce forward propulsive force in situations where lift and drag forces produced by propulsor oscillations cancel and therefore produce no net forward thrust (Daniel, 1984). For *Lepomis* pectoral fin locomotion, several lines of evidence suggest that the acceleration reaction may be particularly important in thrust production. The pectoral fin of *Lepomis* has a Reynolds number (*Re*) of approximately 5×10^3. At Reynolds numbers of this magnitude, hydrodynamic theory predicts that pressure drag and the acceleration reaction are important force components during swimming (see Fig. 3 in Webb, 1988). In addition, the reduced frequency parameter (σ) for the pectoral fin is approximately 0.85. At larger values of σ (σ>0.4), the acceleration reaction dominates force production (Webb, 1988) and unsteady effects cannot be ignored when considering the total force balance on the fin.

At the beginning of abduction–protraction and the end of adduction–retraction in *Lepomis*, there are short periods of rapid fin acceleration and deceleration, respectively (Fig. 9). These periods of rapid change in fin velocity occur when acceleration reaction forces would be predicted to be maximal (Daniel, 1984). As the fin decelerates at the end of abduction, the acceleration force will be an anteriorly directed vector, because the force of the added mass of water around the fin will resist deceleration and tend to move the fish forward. In contrast, at the end of adduction, the added mass of water around the fin will continue to push the fin posteriorly, an action that will also propel the fish forward.

On the basis of the equations and graphical depictions of thrust as a function of appendage angle presented in Daniel (1984), it seems likely that the bluegill fin generates positive, but modest, thrust forces from the acceleration reaction. The stroke angle (γ_1 of Daniel, 1984; Fig. 3) for the bluegill fin is only approximately 60°, whereas a value of 120° is required to maximize acceleration reaction thrust forces for fin strokes which end against the body (γ_2=0, Daniel, 1984). If we assume that the acceleration reaction force acts normal to the pectoral fin, then the acute maximal angle of the fins from the body

results in anterio-laterally directed acceleration reaction force vectors which would have a smaller anteriorly directed thrust component than if the fin were brought out past a 90° angle from the body. However, increasing the angle of the fin from the body would also be likely to increase drag forces greatly. The extent of maximal fin protraction may thus be a compromise between thrust gained from the acceleration reaction and the drag force that opposes movement.

Although we can calculate many of the variables needed to estimate the acceleration reaction (i.e. fluid density, fin volume, acceleration of the fin relative to the fluid), it is extremely difficult to calculate the added mass coefficient of the fin for several reasons. The orientation of the object into the flow has a strong effect on the magnitude of the added mass coefficient. Because the orientation of the fin to the flow changes constantly throughout the fin beat cycle, the added mass coefficient changes as well. If the shape of the object changes during the stroke, then the added mass coefficient will also change. In addition, the large oscillations of the fins may give rise to vortex shedding, a process that will change the added mass coefficient in an unpredictable manner (Daniel, 1984). Thus, although it is clear that the acceleration reaction is important for force production in *Lepomis* pectoral fin swimming, it is difficult to quantify the amount of force it generates.

Blade element theory

It remains unclear how appropriate it is to consider the fin as consisting of a series of straight, rather than curved, elements. As shown in Fig. 10, at the same instant, the orientations of the dorsal and ventral fin elements often differ considerably, particularly at the slowest speed. Hence, the fin surface is actually curved during most of the low-speed swimming movements. During most of fin depression and protraction, the distal edge of the pectoral fin is concave anteriorly and ventrally. During fin retraction and levation, the concavity of the fin surface tends to be oriented posteriorly and slightly ventrally. The paucity of significant phase lags in displacements of markers at speeds greater than $0.3\,\mathrm{TL\,s^{-1}}$ suggests that there is less curvature of the fin at the higher speeds. Hence, the fin may be more plate-like at the higher speeds. In addition to the chordwise curvature of the fin, the fin also curves along the length of the fin rays. Because the coefficients of both lift and drag depend on the shape of an object, the estimates of thrust production for both lift- and drag-based models will be affected by this curvature of the fin.

It is difficult to estimate the flow actually experienced by the pectoral fin. When considering potential mechanisms of lift-based propulsion (Fig. 10), we only considered the distal edge of the fin and we assumed that the incident flow was the vector sum of the overall velocity of the fish plus the velocity of the fin relative to the body of the fish. When flows surrounding flapping structures have been visualized, they often show complex patterns of vortex formation (Brodsky, 1991). Furthermore, as emphasized by Blake (1979), the entire surface of the oscillating structure must be accounted for, and this is computationally complex. For example, the fin tip is motionless relative to the water in the x direction when the retraction speed matches the overall swimming speed; however, the proximal fin will simultaneously experience incident flow equal to the overall swimming speed of the bluegill.

One strategy to increase locomotor efficiency is to increase the proportion of the total

surface area that is located distally in the fin (Blake, 1979). The bluegill pectoral fin does indeed expand substantially proximally to distally. When the fin is at rest against the body of a bluegill with a total length of approximately 18 cm, the distances between the dorsal and ventral edges at the base and the distal tip of the fin are 1.0 and 3.1 cm, respectively. Proceeding from the most proximal to most distal one-third of the fin (based on length of the longest ray), the surface areas are approximately 1.3, 1.6 and 2.4 cm^2, respectively. These areas represent three chordwise strips along the fin span. The combination of within-fin variation in both morphology and three-dimensional kinematics adds to the challenge of attempting to account for all of the forces experienced by the entire fin.

Several results of this study indicate that bluegill sunfish use a type of pectoral fin locomotion which exploits lift, drag and acceleration reaction forces. First, there is no clear pattern of vertical body oscillation or propulsive/recovery phases, as would be expected for purely lift-based or drag-based mechanisms of propulsion, respectively (Fig. 11). Second, there is only a short period during which the speed of retraction of the fin is greater than the overall swimming speed and could potentially be generating forward propulsion by means of drag forces (Fig. 9). Third, the three-dimensional angles of attack, and predictions of lift and force vectors based on these angles, suggest that, although drag forces generate the primary propulsive force during adduction, lift forces may enable bluegill to generate forward thrust during abduction (Fig. 10). Fourth, the reduced frequency parameter and Reynolds number of the pectoral fin (in addition to the pattern of acceleration and deceleration of the fin during the fin beat cycle) indicate that the acceleration reaction is an important component in the generation of force. However, it is important to keep in mind that, to a large extent, these conclusions are contingent on the assumption that subdividing the fin into a series of planar elements creates an accurate hydrodynamic model.

Many critical questions about finned locomotion remain. In particular, there is still a large gap between kinematic studies such as this and the more comprehensive hydrodynamic analyses that are necessary to understand the generation of propulsive forces. In order to bridge this gap, we feel that research could proceed in a number of directions.

First, there is still a dearth of three-dimensional kinematic data on the pectoral fin of fishes during swimming. Further analyses of the movement of the leading edge alone from a ventral view are not likely to add much to current data (Archer and Johnston, 1989; Blake, 1979, 1980; Geerlink, 1983, 1989; Webb, 1973). However, given that kinematic data in three dimensions are only available for one species, it would be useful to obtain such data from several other species swimming at different speeds. Such future work would be particularly valuable if data were to be obtained on a range of speeds in several taxa, some of which typify lift- and drag-based modes of pectoral fin propulsion. The data presented here show complex effects of speed on patterns of fin deformation, and speed by fin element interactions should be a key area for future investigation. In addition, the placement of markers on other areas of the fin (e.g. between the fin base and the distal edge) will allow the fin to be divided into smaller and more precise chordwise units along the span, which could then be analyzed quantitatively using blade element theory. Second, electromyographic studies of the pectoral fin musculature during finned

locomotion may clarify the relationship between active and passive components of fin movement. Third, dye visualization of the flow around the pectoral fin may enable us to assess the extent of vortex shedding around the fin during the fin beat cycle. Finally, the kinematic data obtained here require full treatment in a comprehensive hydrodynamic model such as that of Blake (1983, pp. 234–239). Only by integrating kinematic data with a quantitative model of force production will we be able to understand how thrust is generated by the fin. Such an analysis will probably have to consider the force balance for a number of elements within the fin (the precise number to be determined from kinematic analyses of marked fins) and sum these forces over the entire fin for a series of discrete time intervals during the fin beat cycle.

Support for this work was provided by NSF grant BNS 8919497 to B.C.J. and G.V.L. and NSF BSR 9007994 to G.V.L. The high-speed video system was obtained under NSF BBS 8820664. We thank Professor D. Weihs, Miriam Ashley-Ross, Amy Cook and Gary Gillis for very helpful discussions and the two reviewers for their helpful comments.

References

ALEXANDER, R. MCN. (1989). Optimization and gaits in the locomotion of vertebrates. *Physiol. Rev.* **69**, 1199–1227.

ARCHER, S. D. AND JOHNSTON, I. A. (1989). Kinematics of labriform and subcarangiform swimming in the Antarctic fish *Notothenia neglecta*. *J. exp. Biol.* **143**, 195–210.

BLAKE, R. W. (1979). The mechanics of labriform locomotion. I. Labriform locomotion in the angelfish (*Pterophyllum eimekei*): an analysis of the power stroke. *J. exp. Biol.* **82**, 255–271.

BLAKE, R. W. (1980). The mechanics of labriform locomotion. II. An analysis of the recovery stroke and the overall fin-beat cycle propulsive efficiency in the angelfish. *J. exp. Biol.* **85**, 337–342.

BLAKE, R. W. (1983). Median and paired fin propulsion. In *Fish Biomechanics* (ed. P. W. Webb and D. Weihs), pp. 214–247. New York: Praeger Publishers.

BRODSKY, A. K. (1991). Vortex formation in the tethered flight of the peacock butterfly *Inachis io* L. (Lepidoptera, Nymphalidae) and some aspects of insect flight evolution. *J. exp. Biol.* **161**, 77–95.

CLARK, B. AND BEMIS, W. (1979). Kinematics of swimming of penguins at the Detroit Zoo. *J. Zool., Lond.* **188**, 411–428.

DANIEL, T. L. (1984). Unsteady aspects of aquatic locomotion. *Am. Zool.* **24**, 121–134.

DANIEL, T. L. AND WEBB, P. W. (1987). Physical determinants of locomotion. In *Comparative Physiology: Life in Water and on Land* (ed. P. DeJours, L. Bolis, C. R. Taylor and E. R. Weibel), pp. 343–369. New York: Liviana Press.

GEERLINK, P. J. (1983). Pectoral fin kinematics of *Coris formosa* (Labridae, Teleostei). *Neth. J. Zool.* **33**, 515–531.

GEERLINK, P. J. (1989). Pectoral fin morphology: A simple relation with movement pattern? *Neth. J. Zool.* **39**, 166–193.

GOSLINE, W. A. (1980). The evolution of some structural systems with reference to the interrelationships of modern lower teleostean groups. *Japan. J. Ichthyol.* **27**, 1–28.

GRAY, J. (1968). *Animal Locomotion.* London: Weidenfeld and Nicolson.

HILDEBRAND, M. (1985). Walking and running. In *Functional Vertebrate Morphology* (ed. M. Hildebrand, D. M. Bramble, K. F. Liem and D. B. Wake), pp. 38–57. Cambridge: Harvard University Press.

LINDSEY, C. C. (1978). Form, function and locomotory habits in fish. In *Fish Physiology*, vol. 7 (ed. W. S. Hoar and D. J. Randall), pp. 1–100. New York: Academic Press.

NACHTIGALL, W. (1966). Die kinematik der Schlagflügelbewegungen von Diptereni Methodische und analytische Grundlagen zur Biophysik des Insektenflugs. *Z. vergl. Physiol.* **52**, 155–211.

WEBB, P. W. (1973). Kinematics of pectoral fin propulsion in *Cymatogaster aggregata*. *J. exp. Biol.* **59**, 697–710.

WEBB, P. W. (1975). Hydrodynamics and energetics of fish propulsion. *Bull. Fish. Res. Bd Can.* **190**, 1–158.

WEBB, P. W. (1988). Simple physical principles and vertebrate aquatic locomotion. *Am. Zool.* **28**, 709–725.

WEBB, P. W. (1993). The effect of solid and porous channel walls on steady swimming of steelhead trout, *Oncorhynchus mykiss*. *J. exp. Biol.* **178**, 97–108.

WEBB, P. W. AND BLAKE, R. W. (1985). Swimming. In *Functional Vertebrate Morphology* (ed. M. Hildebrand, D. M. Bramble, K. F. Liem and D. B. Wake), pp. 110–128. Cambridge: Harvard University Press.

WINTERBOTTOM, R. (1974). A descriptive synonymy of the striated muscles of the Teleostei. *Proc. natn. Acad. Sci. U.S.A.* **125**, 225–317.

ZAR, J. H. (1984). *Biostatistical Analysis*. Englewood Cliffs: Prentice-Hall.